

Original Article

# Aerodynamic Aspects in the Formation of the Appearance of Mainline Aircraft at the Preliminary Design Stage

Aleksandr Gorbunov<sup>1</sup>, Aleksei Pripadchev<sup>2</sup>, Aleksandr Magdin<sup>3</sup>, Elena Ezerskaya<sup>4</sup>

<sup>1,2,3,4</sup>Orenburg State University, Orenburg, Russia.

<sup>1</sup>Corresponding Author : [aleksandr.a.gorbunov@mail.ru](mailto:aleksandr.a.gorbunov@mail.ru)

Received: 17 February 2023

Revised: 05 April 2023

Accepted: 09 May 2023

Published: 25 May 2023

**Abstract** - The study focuses on the improvement of mainland aircraft aerodynamics. The paper presents a study of the mechanism of the formation of induced drag for a finite-span wing. The authors propose a possible option of considering circulation value as a control parameter in the preliminary design of the wings of mainland aircraft equipped with wingtips. The research results may serve as a basis for the conceptual model, mathematical software, and application software implementing the methodology for selecting the composition of rational engineering parameters. The implementation of these findings could lead to increased fuel efficiency, reduced emissions, and overall better performance of mainland aircraft, contributing to a more sustainable and efficient aviation sector.

**Keywords** - Additional aerodynamic surfaces (Wingtips, Winglet), Airplane appearance, Choice of parameters, Element design, Vector of parameters.

## 1. Introduction

Considering directions for improving the aerodynamics of mainline aircrafts, with an adequate approach (from the point of the logic of design solution synthesis), considerable changes in aircraft performance can be achieved [1- 4]. These improvements include the reduction of aerodynamic resistance at cruising flight modes from 10 to 20%, decreasing specific fuel consumption, and a lower required takeoff distance with the full commercial load [5- 7]. Improvement of aerodynamics is understood as a change in appearance characteristics (geometric shape and relative positioning of mainline aircraft units) of the system of bearing surfaces, including the wing and the fins. Given that the fin is a means of aerodynamic balancing for the mainland aircraft of the classical aerodynamic scheme, the greatest effect is achieved through modifications and modernization of the wing [8- 10]. Modern practice and scientific research show that the use of additional aerodynamic surfaces (AAS) (wingtips, winglet) increases the aerodynamic efficiency of the aircraft, leading to lower fuel consumption [11-13]. While the benefits of AAS have been widely recognized and implemented in the aviation industry, there is still potential for further research and development to maximize their efficiency and effectiveness. Developing AAS that can adapt to different flight conditions or phases, such as takeoff, cruise, and landing, could improve efficiency across various flight scenarios.

This ongoing investigation will contribute to the continuous improvement of aircraft performance and sustainability. The present study aims to identify the most significant aerodynamic aspects in the formation of the appearance of mainland aircrafts at the stage of preliminary engineering. The design of mainland aircraft wings at the design stage of its elements can be presented as the interconnected process of finding the required characteristics for the selected efficiency criterion. The efficiency criterion at this stage is the resolution of the optimization task to minimize the relative wing mass.  $\underline{m}_w$ , expressed as a target function  $f_0^2 = \underline{m}_w \rightarrow \min$ . Limitations, in this case, include flight distance  $L_p$  and wing load  $p_0$ , Mach number in cruise flight mode  $M_{cr}$ , and final approach speed  $V_{f.a.}$ . The variables are the coefficients of drag  $C_x$  and lift  $C_y$ , the value and nature of circulation  $G$ , effective wing elongation  $\lambda_{ef.}$ , wing narrowing  $\eta$ , quarter chord wing sweep angle  $\chi$ , wing area  $S_w$ , the mass of the aircraft in first approximation  $m_0$ , and the allowable stress value in the structural elements at a given structural and power scheme  $\sigma$ , (Figure 1). The controlling parameters are AAS, which affects the nature of changes in circulation  $G$  along the wingspan, which leads to a change in the dimensionless coefficients.  $C_x$  and  $C_y$ . The output is a parameterized plan view of the wing.



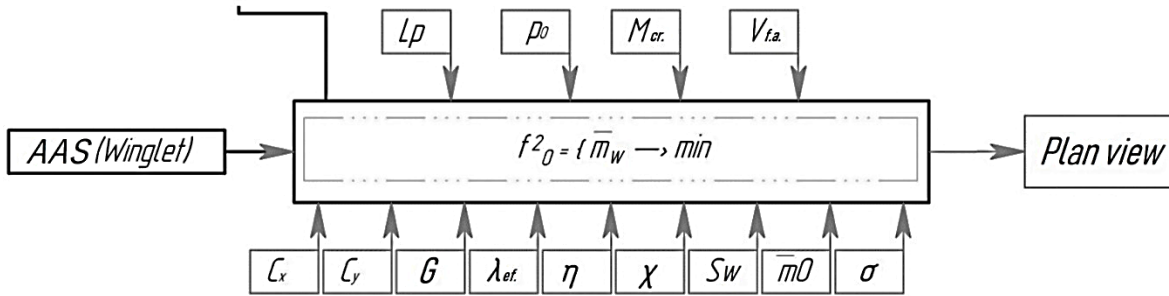


Fig. 1 Design of mainline aircraft elements, "Wing + AAS"

**2. Methods**

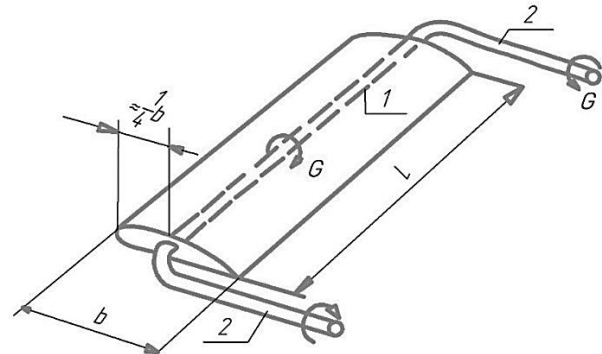
From the point of view of aerodynamic design, the wing can be replaced by a wing of infinite span in the first approximation in the form of an infinitely long concentrated vortex, which is called an attached wing vortex. Since the value of induced drag for an infinite span wing does not exist, a finite span wing has no unambiguous (defined) point of application. Its value cannot be precisely determined without experimental research methods; at the stage of design of aircraft elements, it is advisable to use a coefficient obtained through research and development.

A finite span wing cannot have only an attached finite vortex, as it would contradict the Helmholtz vortex theorem, by which a vortex cannot be interrupted in a fluid (in this case, on the wing ends). Therefore, as an approximate model, a finite span wing can be replaced by one attached vortex with two tails, wherein the attached vortex should be within the wing, and the tails, called free vortices, should extend beyond the wing at the ends and, picked up by the flow, extend to infinity.

For a finite-span wing, the flow is not plane-parallel but spatial, especially near its ends. The ends of the wing affect the distribution of pressure over its entire surface. Thus, a finite span wing can be replaced by one infinite concentrated vortex that is not straight but U-shaped (horseshoe) in the plan (Figure 2). The presence of free concentrated vortices stretching behind a finite span wing is detected by experiments

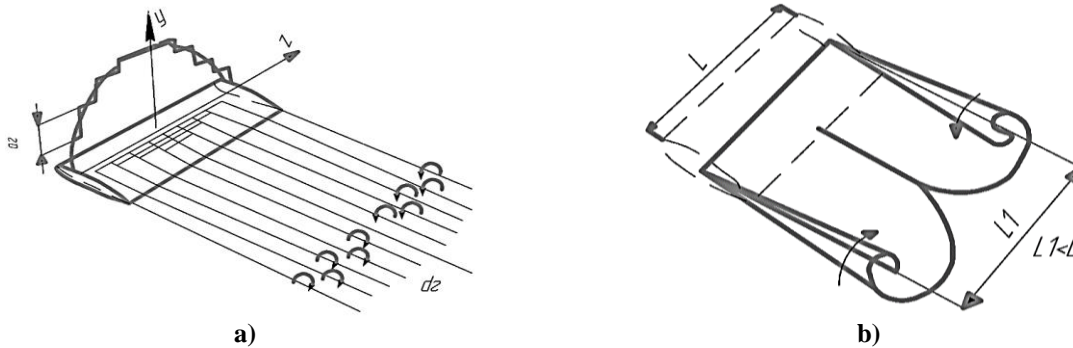
in wind tunnels with tufts or smoke. It should be noted that in the adopted simplest vortex scheme, the circulation along the wing of a finite span was assumed to be constant. However, experience has shown that circulation along the wingspan varies [14-16].

Specifically, circulation reaches its maximum in the center of a rectangular wing and the minimum at the ends. To keep the adopted scheme for the circulation variable, instead of one U-shaped concentrated vortex, the wing can be replaced by a system of U-shaped vortex filaments.



1 – attached vortex; 2 – free vortex  
Fig. 2 Vortex diagram of a finite span wing:

Along each such vortex filament, the circulation will be constant, but when passing from one wing section to another, the circulation will change in a spasmodic manner (Figure 3).



a – vortex sheet; b – curtailed vortex sheet  
Fig. 3 Finite span wing diagram

For circulation along the wing to be changing continuously, we can assume that the number of horseshoe vortices tends to change to infinity. In this case, behind the wing, the free vortices merge into a single whole and form a vortex sheet composed of an infinitely large number of vortex filaments coming off the wing. Research of the vortex sheet behind the wing indicates that it is unstable, and shortly after coming off, the wing curls into two conically shaped concentrated vortices. This fact is not considered in the theory of a finite span wing because it is very difficult to account for from a mathematical point of view [25,26].

### 3. Calculation Formula

Any bearing body, including a wing, is subject to a lifting force from the fluid, usually directed upward. The reaction of the wing is directed downward. Under the finite-span wing, an increased pressure (underpressure) is created, and above the wing, there is a reduced pressure (suction). The pressure difference causes the air to move downward. However, near the wing ends, the air, on the contrary, rises upward. In addition, the values of rarefaction and increased pressure change with distance from the wing symmetry axis. This pressure changes lead to transverse currents directed from higher to lower pressures.

The end-free vortices are generated by air flowing from the lower side of the wing from the area of higher pressure to the area of rarefaction on the upper side of the wing. These air movements near the wing are superimposed on the forward flow and deflect downward. Thus, with the wing of a finite span, there is a bevel of the flow (Figure 4).

The bevel angle  $\Delta\alpha$  depends on the value of vertical velocity,  $v_y$ , induced by the wing. Since this angle is typically small, the relationship can be presented in the form calculated by the formula:

$$tg\Delta\alpha \approx \Delta\alpha = \frac{v_y}{v_\infty} \tag{1}$$

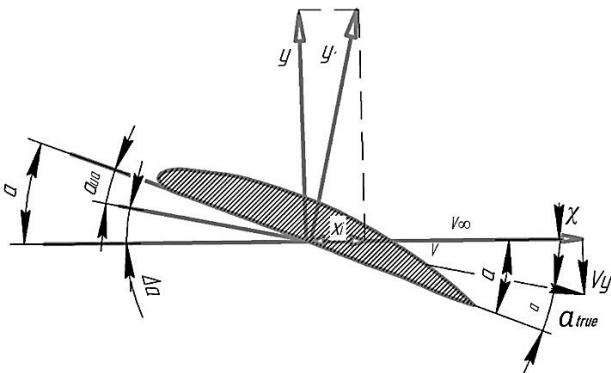


Fig. 4 Triangles of velocities and forces in an infinite span wing equivalent to a finite span wing

Due to the flow level, the actual angle of attack of the wing will differ from the geometric angle of attack by the value of  $\Delta\alpha$  calculated by the formula:

$$\alpha_{true} = \alpha - \Delta\alpha = \alpha - \frac{v_y}{v_\infty} \tag{2}$$

Rotation of the velocity vector of the incoming flow by the angle of  $\Delta\alpha$  causes the same rotation of the lifting force vector,  $Y$ . However, from the point of flight dynamics, the actual lifting force is not the entire force of  $Y$ , but its component normal for the direction of undisturbed flow calculated by the formula:

$$Y = Y \cdot \cos\Delta\alpha \approx \underline{Y} \Rightarrow X_i = Y = \underline{Y} \cdot tg\Delta\alpha \approx Y\Delta\alpha \tag{3}$$

The force of  $X_i$  is directed along the flow in the direction opposite to the wing movement and is called induced drag. Thus, a finite-span wing has a special kind of resistance due to the effect of wing ends due to the beveling of the flow. This resistance is related neither to viscosity or friction nor to flow disruption, meaning that a finite span wing will have induced drag even in an ideal fluid.

### 4. Stages of the Study

The characteristics of the aerodynamic aircraft model for different airflow conditions were determined by a series of tests using two subsonic wind tunnels (ATD T-1 OGU and ADT T-3 SGAU) of continuous operation with an open working part, closed type, with an automated data processing and storage system. In the conducted experimental studies, full geometric similarity for the aerodynamic aircraft models was ensured (Figure 5). The equality of dimensionless coefficients in the conducted experiment is impossible due to the operating characteristics of the wind tunnels; therefore, the principle of conditional similarity, i.e., the principle of self-similarity, was used [19].

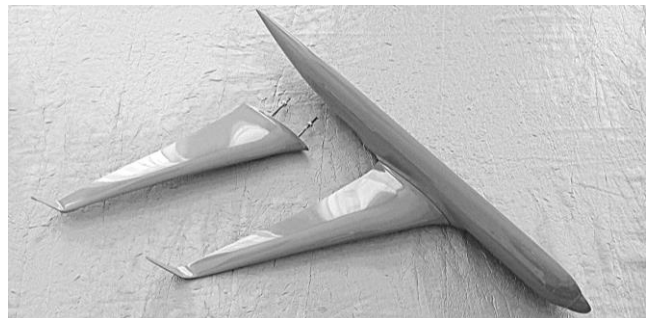
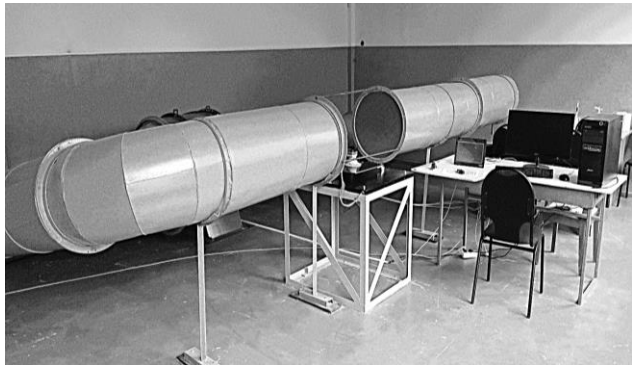


Fig. 5 Aerodynamic model of the arrangement of main aircraft elements "Fuselage+Wing+AAS"

The information and measurement system (IMS) of subsonic wind tunnels is a multichannel measurement structure based on the Omron multichannel programmable

controller for ATD T-1 OGU and L-1250 for ATD T-3 SGU, programmable logic controllers, as well as a set of software and hardware with a block-module structure and a universal computing core. The processor provides input of analog information, its analysis in a computer-independent mode, and subsequent reporting of the analysis results. The IMS is controlled from the computer via special software drivers with CJ2M programmable logic controllers [20].

Aerodynamic balance for the two wind tunnels used is a device containing strain gauge transducers of non-electrical values (elastic deformations) into an electrical signal. The balance allows measuring loads by the components  $X$ ,  $Y$ ,  $Z$ ,  $M_x$ ,  $M_y$ , and  $M_z$  in the coordinate system associated with the model. The output voltages are fed to the amplifiers.



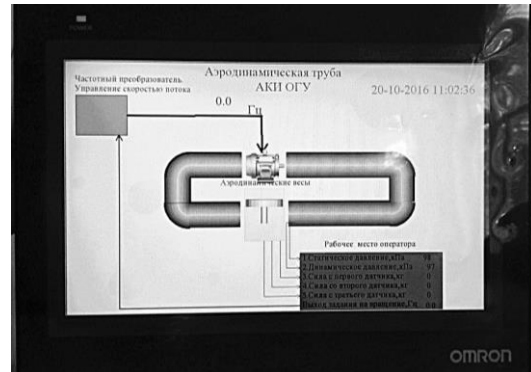
a) general view

The main varying parameters in the experiment were the installation angles of the aerodynamic model, the values equaling  $-10^0$ ,  $-8^0$ ,  $-6^0$ ,  $-4^0$ ,  $-2^0$ ,  $0^0$ ,  $2^0$ ,  $4^0$ ,  $6^0$ ,  $8^0$ , and  $10^0$ , respectively. The flow rate changed for each installation angle of the models, which amounted to 10 m/s, 15 m/s, 20 m/s, 25 m/s, and 30 m/s.

Using the built-in IMS tools, it is possible to specify the time step for displaying the incoming parameters from the aerodynamic balance and for the output of the information in the form of histograms and graphs (Figure 6).

## 5. Results and Discussion

Further post-processing of the results of weight tests demonstrates an insignificant variation of the experimental data within 7%.



b) control terminal

Fig. 6 Aerodynamic tube ADT T-1

The conducted weight tests indicate the dimensionless aerodynamic coefficients for different angles of attack and flow velocities. The results of balance tests are systematized and arranged by blowout speeds and model installation angles.

In the example of the "Fuselage+Wing+AAS" element arrangement, the following is observed. The physical meaning of applying AAS is to change the value of effective wing elongation. The geometric interpretation of change in the value of effective elongation looks like an equivalent

wing with a comparable area but a larger span, where  $S_1 = S_2$  and  $\lambda_{ef. 2} > \lambda_{ef. 1}$ .

The wing design should achieve an elliptical distribution of lift and circulation along the span, but in practice, the following characteristic pattern is observed (Figure 7). The aircraft fuselage influences the law of circulation distribution, and the nature of its influence on a given aerodynamic scheme is almost impossible to change. Nevertheless, it is possible to increase the magnitude of lift on the wing ends by equipping it with AAS.

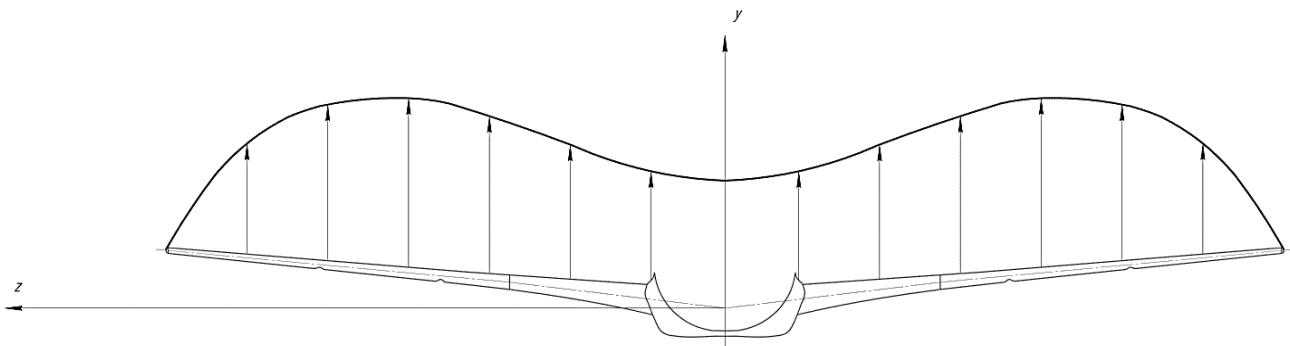


Fig. 7 Distributions of lift force along the wingspan of a mainline aircraft without AAS

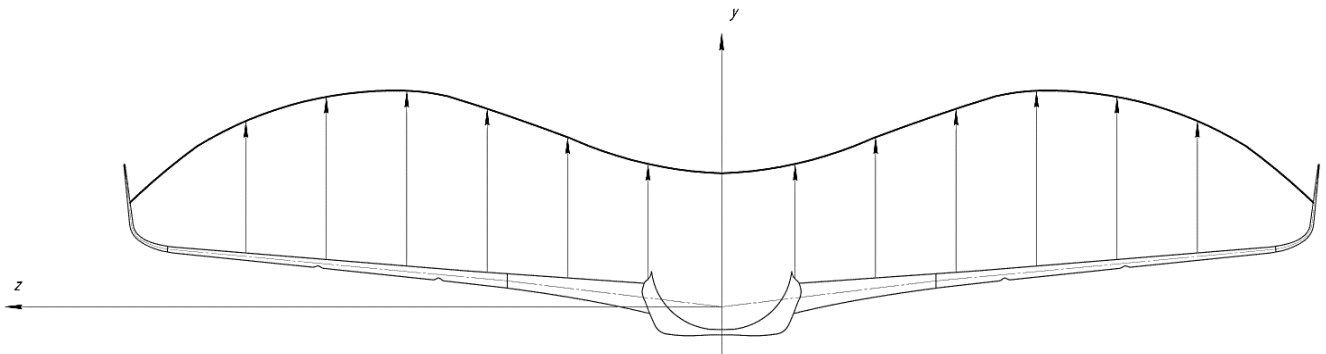


Fig. 8 Distributions of lift along the wingspan of a mainline aircraft with AAS, type "Krylyshko"

Examining the distribution of lift and its pattern of change along the wingspan of a wing equipped with AAS (Figure 8), we observe a noticeable increase in the value of lift at the wing end, with the circulation value  $G$  taking an almost elliptical form.

This process of distribution of circulation  $G$  is due to the nature of the flow processes of a swept wing of large elongation  $\lambda > 5$  at high subsonic flight speeds with  $M \leq 1$ . The aerodynamic design of a wing requires the fulfillment of several requirements, which can be formed as follows: ensuring the lowest possible aerodynamic drag; providing the maximum possible lifting force throughout the flight profile; ensuring longitudinal and transverse stability and controllability [21, 22].

When wing elongation is reduced, the effect of overflow at the wing ends increases, and the presence of a sweep contributes to the overflow of pressure along the leading edge of the wing [27]. As a result of the interaction of current lines in the places of pressure overflow, a vortex sheet is formed behind the trailing edge of the wing, and a powerful tip vortex is formed on the end parts. This pattern of circulation  $G$  generates a harmful resistance called induced drag  $C_{xi}$ . Ultimately, the deviation of current lines from the general flow of air around the wing leads to a change in the vector of lift  $C_y$  due to its tilting by a certain angle. The characteristic picture of the flow circulation along the wingspan of a mainline aircraft without AAS is shown in Figure 9. The X-axis is directed in the direction of flight.

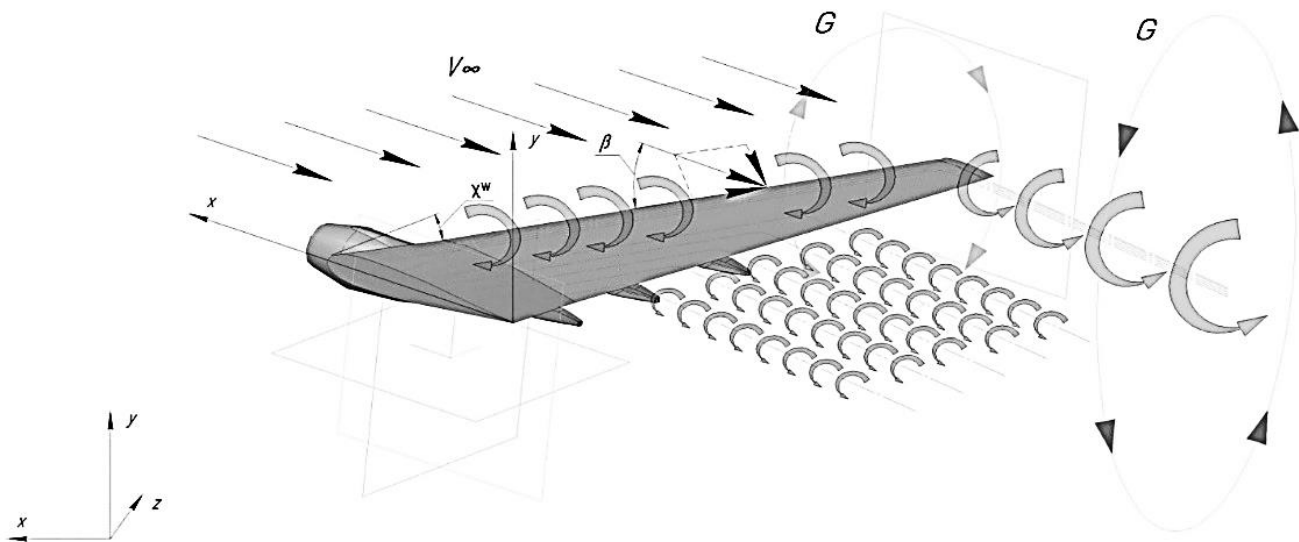


Fig. 9 The pattern of infinite flow around the wing of a mainland aircraft without AAS with a velocity of  $V_\infty$

Various types of AAS allow for partially preventing and localizing the process of pressure transfer near the end part of the wing, as well as changing the flow pattern around a finite-span wing. For the AAS of the type "Krylyshko", the current lines along the wingspan take on the form presented in Figure 10. Tilting of the lifting force vector  $C_y$  is not fully

compensated by the use of AAS, yet changes in the vector and partial localization of current lines at the end part of the AAS weaken the powerful tip vortex. The value of induced drag decreases, which leads to a higher value of effective elongation of the wing, and as a consequence, better aerodynamic quality and decreased drag  $C_x$ .

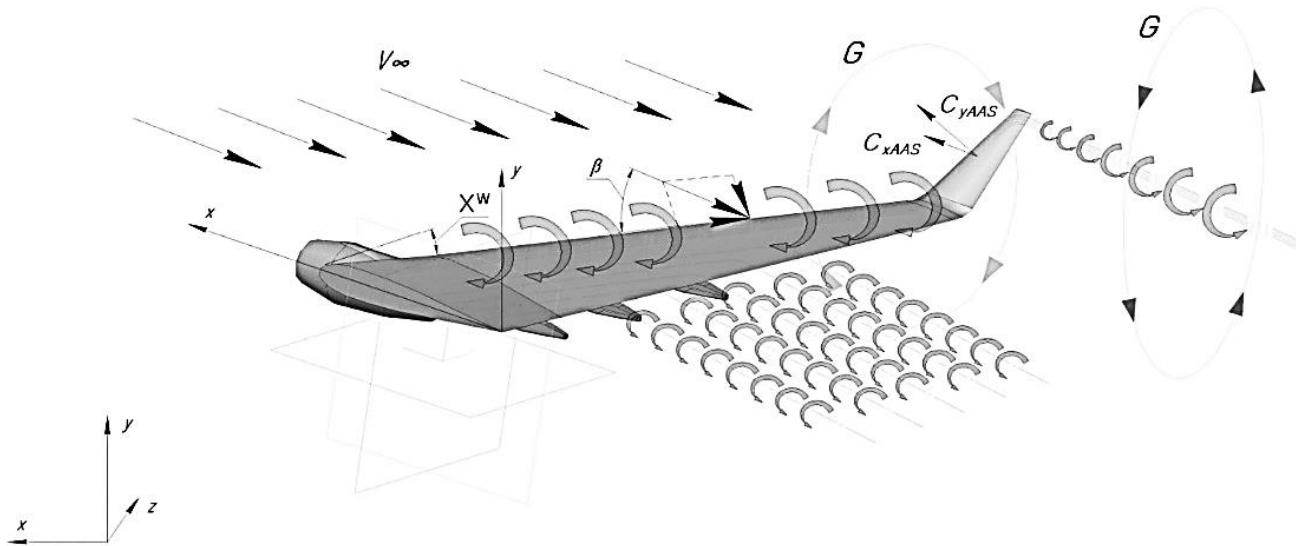


Fig. 10 The pattern of infinite flow around the wing of a mainline aircraft with AAS of the type "Krylyshko" with a velocity of  $V_\infty$ .

The characteristic flight profile (trajectory or cyclogram) for a mainline aircraft assumes a long flight at high subsonic speeds with  $M \leq 1$  and a relatively small angle of attack. Under such conditions (modes of operation), part of the resistance of the wing is determined by friction resistance [24]. The pressure resistance at a relatively small value of the wing profile thickness is significantly lower. Therefore, to ensure the lowest possible friction resistance, it is advisable to provide the maximum possible smoothness of the wing surface and apply the profile with the longest laminar segment of the boundary layer. When the critical value of  $M$  is approached, supersonic zones appear on the wing, leading to the occurrence of wave drag, so it is vital to delay the occurrence of the wave crisis as long as possible. For this reason, the glide effect is used for finite-span swept wings.

Since it is impossible to obtain the lift of a finite-span wing without induced drag, the latter constitutes a measure of the energy expended to create lift. Indeed, if we imagine that the lift is created by air masses being thrown down by the wing, then the lift should equal the amount of motion of these discarded masses. Continuous downward deflection of air masses requires a power equal to the product of the force by the speed of flight, the force, in this case, being the force of induced drag.

For a given lifting force and, therefore, a given amount of air thrown downward, discarding a larger mass at a slower velocity is more energetically efficient. At a given flight speed, greater mass can be discarded only with a large wingspan, i.e. capturing a large volume of air. Consequently, to reduce induced drag, it is more advantageous to have a large wingspan or a large relative elongation and fly at high speed and use the so-called AAS. The effect of the wingtips delaying overflow at the ends of the wing increases the

effective span, i.e. the wing acquires a new effective elongation greater than the geometric one.

## 6. Conclusion

The study's theoretical significance is provided by the fact that the obtained experimental data and functional relationships serve as a basis for the formal aerodynamic model linking the geometry of the aircraft model (appearance) and its aerodynamic characteristics through dimensionless coefficients at different operating conditions. The practical applicability of the results is supported by the fact that they have been adopted in the design and development activities of major state-owned companies in the aviation industry.

The presented research results formed the basis of the conceptual model, mathematical software, and application software implementing the methodology for selecting the composition of rational engineering parameters, which provides a commonality in terms of the integration of parameters considered in assessing the effectiveness of the aircraft under the same operating condition, invariant to the type of aircraft and its components. The use of the C++ programming language will enable the integration of the developed software into the aviation and defense industry cluster enterprises.

## Funding Statement

The work was carried out within the framework of the scholarship of the President of the Russian Federation No. SP-1811.2021.1 dated 29.12.2020 for young scientists and postgraduates to perform a scientific study on the topic "Expanding the information groundworks of the technology of forming the conceptual parameters of the next generation of aircraft".

## References

- [1] G. Corrado et al., "Recent Progress, Challenges and Outlook for Multidisciplinary Structural Optimization of Aircraft and Aerial Vehicles," *Progress in Aerospace Sciences*, vol. 135, pp. 100861, 2022. [[CrossRef](#)] [[Google Scholar](#)] [[Publisher Link](#)]
- [2] Yuping Wang et al., "Aerodynamic Performance of the Flexibility of Corrugated Dragonfly Wings in Flapping Flight," *Acta Mechanica Sinica/Lixue Xuebaom*, vol. 38, no. 11, 2022. [[CrossRef](#)] [[Google Scholar](#)] [[Publisher Link](#)]
- [3] J.E. Guerrero, M. Sanguineti, and K. Wittkowski, "Variable Cant Angle Winglets for Improvement of Aircraft Flight Performance," *Meccanica*, vol. 55, no. 10, pp. 1917-1947, 2020. [[CrossRef](#)] [[Google Scholar](#)] [[Publisher Link](#)]
- [4] Wengang Chen et al., "Shape Optimization to Improve the Transonic Fluid-Structure Interaction Stability by an Aerodynamic Unsteady Adjoint Method," *Aerospace Science and Technology*, vol. 103, 2020. [[CrossRef](#)] [[Google Scholar](#)] [[Publisher Link](#)]
- [5] Gang Wang et al., "Deployment Modes and Aerodynamic Analysis of UAV Orthogonal Biaxial Folding Wing," *Aerospace*, vol. 10, no. 1, p. 26, 2023. [[CrossRef](#)] [[Google Scholar](#)] [[Publisher Link](#)]
- [6] Hiroki Mukohara, and Masayuki Anyoji, "Computational Analysis of Compressibility Effect on Flow Field and Aerodynamics at Low Reynolds Numbers," *Physics of Fluids*, vol. 34, no. 51, 2022. [[CrossRef](#)] [[Google Scholar](#)] [[Publisher Link](#)]
- [7] Shiva Prasad Uppu et al., "High-Speed Flow Over Airfoils, Wings and Airplane Configurations," *Handbook of Research on Aspects and Applications of Incompressible and Compressible Aerodynamics*, pp. 230-254, 2022. [[CrossRef](#)] [[Google Scholar](#)] [[Publisher Link](#)]
- [8] Chukwugozie Ejeh et al., "Investigating the Impact of Velocity Fluctuations and Compressibility to Aerodynamic Efficiency of a Fixed-Wing Aircraft," *Results in Physics*, vol. 18, 2020. [[CrossRef](#)] [[Google Scholar](#)] [[Publisher Link](#)]
- [9] Shuichi Hiramatsu et al., "Aeroelastic Deformation Measurement of Martian Airplane for High-Altitude Flight Experiment Using Stereophotogrammetry," *Engineering Research Express*, vol. 3, no. 1, 2021. [[CrossRef](#)] [[Google Scholar](#)] [[Publisher Link](#)]
- [10] Like Xie et al., "Improving Aircraft Aerodynamic Performance with Bionic Wing Obtained by Ice Shape Modulation," *Chinese Journal of Aeronautics*, vol. 36, no. 2, pp. 76 – 86, 2023. [[CrossRef](#)] [[Google Scholar](#)] [[Publisher Link](#)]
- [11] Ignazio Dimino, "Integrated Design of a Morphing Winglet for Active Load Control and Alleviation of Turboprop Regional Aircraft," *Applied Sciences*, vol. 11, no. 5, pp. 127, 2021. [[CrossRef](#)] [[Google Scholar](#)] [[Publisher Link](#)]
- [12] I. B. Manjunath, V. M. Kulkarni, and P. Balaraman, "Geometry Optimization Studies on Nonplanar Wingtip Devices for Typical Transport Aircraft," *Journal of Physics: Conference Series*, vol. 1473, no. 1, 2020. [[CrossRef](#)] [[Google Scholar](#)] [[Publisher Link](#)]
- [13] C. Conlan-Smith et al., "Aerodynamic Shape Optimization of Aircraft Wings Using Panel Methods," *American Institute of Aeronautics and Astronautics Journal*, vol. 58, no. 9, pp. 3765-3776, 2020. [[CrossRef](#)] [[Google Scholar](#)] [[Publisher Link](#)]
- [14] Hadar Ben-Gida, and R. Gurka, "The Leading-Edge Vortex Over a Swift-Like High-Aspect-Ratio Wing with Nonlinear Swept-Back Geometry," *Bioinspiration and Biomimetics*, vol. 17, no. 6, 2022. [[CrossRef](#)] [[Google Scholar](#)] [[Publisher Link](#)]
- [15] M. A. Poghosyan, Ed., *Proektirovanie Samoletov, Aircraft Design*, Moscow, Russia: Innovacionnoe Mashinostroenie, 2018.
- [16] D. P. Raymer, *Aircraft Design: A Conceptual Approach*, Aerospace Research Central, 1992.
- [17] Pratheepan J., and Bruce Ralphin Rose, J., "Aileron Effectiveness in the Presence of Aeroelastic Deformations," *SSRG International Journal of Mechanical Engineering*, vol. 2, no. 6, pp. 12-16, 2015. [[CrossRef](#)] [[Google Scholar](#)] [[Publisher Link](#)]
- [18] Nishant Kumar, Saurav Upadhaya, and Ashish Rohilla, "Evaluation of the Turbulence Models for the Simulation of the Flow Over a Tsentralniy Aerogidrodinamicheskoy Institut (TsAGI)-12% Airfoil," *SSRG International Journal of Mechanical Engineering*, vol. 4, no. 1, pp. 18-28, 2017. [[CrossRef](#)] [[Google Scholar](#)] [[Publisher Link](#)]
- [19] I. A. Belov et al., *Problems and Methods for Calculating Separated Flows of an Incompressible Fluid*, Leningrad, USSR: Sudostroenie, 1989.
- [20] V. T. Kalugin et al., *Aerodinamicheskie Truby Dozvukovykh i Sverkhzvukovykh Skorostej, Aerodynamic Tubes of Subsonic and Supersonic Velocities*, Moscow, Russia: Publishing House of Bauman Moscow State Technical University, 2004.
- [21] S. Khan, and S. Sharma, "Analysis of Cloud Computing for Security Issues and Approaches," *International Journal on Emerging Technologies*, vol. 10, no. 1, pp. 68-73, 2019. [[Google Scholar](#)] [[Publisher Link](#)]
- [22] Victor Maldonado et al., "Active Flow Control as a Technique To Improve Fixed-Wing and Rotary-Wing Aerodynamics of Uavs," *AUVSI XPONENTIAL 2020*, 2020. [[Google Scholar](#)] [[Publisher Link](#)]
- [23] Md Rafiqur Rahman, "Computational Analysis of Aerodynamic Parameters for Supersonic Artillery Projectiles," *SSRG International Journal of Mechanical Engineering*, vol. 7, no. 8, pp. 5-17, 2020. [[CrossRef](#)] [[Google Scholar](#)] [[Publisher Link](#)]
- [24] M. Zhao et al., "Dynamic Stall of Pitching Tubercled Wings in Vortical Wake Flowfield," *Physics of Fluids*, vol. 35, no. 1, 2023. [[CrossRef](#)] [[Google Scholar](#)] [[Publisher Link](#)]
- [25] A. G. Bratuhin, Ed., *Mezhdunarodnaya Enciklopediya CALS. Aviacionno-Kosmicheskoe Mashinostroenie* [International Encyclopedia CALS. Aerospace Engineering]. Moscow, Russia: NIC ASK, 2015.
- [26] K. P. Petrov, *Aerodinamika Elementov Letatelnykh Apparatov* [Aerodynamics of Aircraft Elements]. Moscow, USSR: Mashinostroenie, 1985. [[Google Scholar](#)]
- [27] Hyounjin Kim, and May-Fun Liou, "Flow Simulation and Drag Decomposition Study of N3-X Hybrid Wing-Body Configuration," *Aerospace Science and Technology*, vol. 85, pp. 24 – 39, 2019. [[CrossRef](#)] [[Google Scholar](#)] [[Publisher Link](#)]